Desalination and Water Treatment
www.deswater.com

doi: 10.5004/dwt.2017.21425

88 (2017) 207–220
September

Evaluation of nanosilica, extracted from stem sweep, as a new adsorbent for simultaneous removal of crystal violet and methylene blue from aqueous solutions

M. Ashrafi, M. Arab Chamjangali, G. Bagherian*, N. Goudarzi, S. Kavian

College of Chemistry, Shahrood University of Technology, Shahrood, P.O. Box 36155-316, Iran,
email: mot.ashrafi@gmail.com (M. Ashrafi), arabe51@yahoo.com (M.A. Chamjangali), Tel. +98 23 32395441,
email: Gh_Bagherian@shahroodut.ac.ir (G. Bagherian), goudarzi10@yahoo.com (N. Goudarzi), safura.kavian @gmail.com (S. Kavian)

Received 4 March 2017; Accepted 8 September 2017

ABSTRACT

In this work, nanosilica was extracted from stem sweep and used as a new adsorbent for the simultaneous removal of the crystal violet (CV) and methylene blue (MB) dyes in a batch mode. The influence of the experimental variables including the solution pH, adsorbent dosage, initial dye concentration, and contact time on the adsorption process was studied. Analysis of the equilibrium data revealed that adsorption of the understudied dyes in single and binary systems can be fitted to the Langmuir and the extended-Langmuir isotherms, respectively. Kinetic investigations carried out on the CV and MB removal suggested that the adsorption processes followed a pseudo-second order kinetics rate. For the first time, a modeling of the simultaneous removal of CV and MB on the prepared adsorbent was presented using the random forest (RF) and multiple linear regression (MLR) methods. The random forest (RF) model, recognized as a reliable and powerful computational technique, was used to predict the removal percentage of the cited dyes in a binary mixture as a function of the experimental parameters. The mean square errors (MSEs) and squared correlation coefficients (R^2s) for CV were 3.29 and 0.9754, respectively, and those for MB were 2.41 and 0.9781, respectively. These results confirm the ability and accuracy of the proposed RF model (with respect to the multiple linear regression method) for estimating the behavior of the adsorption processes under different experimental conditions. For the first time, a dish-washing liquid was used, as a cheap and available solvent, for the regeneration of the proposed adsorbent.

Keywords: Stem sweep; Derivative spectrophotometry; Nanosilica; Random forest

1. Introduction

Synthetic dyes are an important class of organic compounds widely used in different industries in order to dye the materials such as textile, leather, paper, pulp, and plastic [1]. Approximately, 7×10^5 to 1×10^6 tons of dyes are produced annually [1,2]. Relatively large amounts (10–20%) of these products are lost due to incomplete exhaustion, which produce a large amount of dye-containing wastewater [3]. Among these synthetic dyes, crystal violet (CV) and methylene blue (MB) are two kinds of cationic dyes that are widely used in different fields. CV, as a dye belonging to the triarylmethane class, is used in manufacturing paint and printing ink, paper, leather, silk, and wood industries, and as a biological stain and a dermatological agent in medical community [3,4]. On the other hand, MB is a thiazine dye, which is used as a redox indicator in chemistry laboratories, and as the dyestuff used for dying cotton, wood, paper, and silk [5]. In spite of their wide applications, these colored compounds have several drawbacks. They can reduce the sunlight transmission into water, and can thus affect photosynthesis [6]. Moreover, they can cause harmful effects such as gene mutations, allergic dermatitis, and cancer [4,7]. Therefore, removing these dyes from the effluents containing these compounds before delivering them into the natural environment is essential [8]. Different methods such as coagulation, flocculation, electrolysis, ozonation, and adsorption have been utilized for the treatment of

*Corresponding author.

dyestuff wastewater [6,7,9]. Of these, the adsorption-based separation procedure using eco-friendly materials has been considered to be superior to the other techniques due to its design, simplicity, and availability of different adsorbents [6,10]. The most commonly used adsorbent for the removal of these dyes from wastewater is the activated carbon [5]. However, a major challenge for the adsorption process is the high production cost of the activated carbon [4,11,12]. Recently, efforts have been made to use the available and cut-price materials such as waste materials from industry and agriculture for the removal of dyes [5,13–15]. Agricultural wastes have proved to be of greatest importance due to their availability. For this reason, in this work, we used nanosilica, extracted from stem sweep, as a low-cost adsorbent for removal of the dyes. Stem sweep is one of the abundantly available agricultural waste materials containing a high amount of nanosilica that can be used as a nanosilica source. In comparison with other agricultural wastes such as rice husk that is more commonly used, stem sweep has a little economic value and is inappropriate to be utilized as animal and poultry feeds due to its hardness. Therefore, it is desirable to use it as a low-cost source for the preparation of an adsorbent that can be used for removal of dyes. Although commercial silica is used for the removal of MB from a single system [16], in real wastewater systems, there is a mixture of dyes affecting the dye-adsorption behavior. The aim of this work was to investigate the performance of nanosilica, extracted from stem sweep, for the simultaneous removal of the CV and MB dyes from single and binary systems. To the best of our knowledge, there is no report on the application of nanosilica, extracted from stem sweep, for the competitive removal of the dyes or metals present in single and binary systems.

It should be noted that modeling an adsorption process permits to evaluate the influence of each factor involved and simulate the removal efficiency with fewer experiments [17]. Modeling is a simplification of reality, being very appropriate for investigating the behavior of each process [18]. Recently, reliable and powerful computational methods such as artificial neural networks (ANNs) and random forest (RF) have been used to model an adsorption process [17,18].

The objectives of the present work were as follow. (a) Extraction of nanosilica from stem sweep and its characterization using FT-IR spectroscopy and scanning electron microscopy (SEM). (b) Assessment of the adsorptive potential of nanosilica for the elimination of dyes from aquatic environments. (c) Estimating the removal percentage of the mentioned dyes as a function of the experimental parameters using the computational techniques such as RF and MLR. (d) Examination of the isotherms and kinetics of the adsorption process. (e) Evaluation of the recovery of the proposed adsorbent.

2. Experimental

2.1. Materials, instruments, and software

Stem sweep (Fig. 1A) was collected from a local field in Shahrood, Iran. Hydrochloric acid and sodium hydroxide, with the highest purity available, were supplied from Merck. The CV and MB dyes were obtained from Merck and used without further purification. The stock solution of each dye (0.500 g L^{-1}) was prepared, and the working solutions were prepared by successive dilutions to the

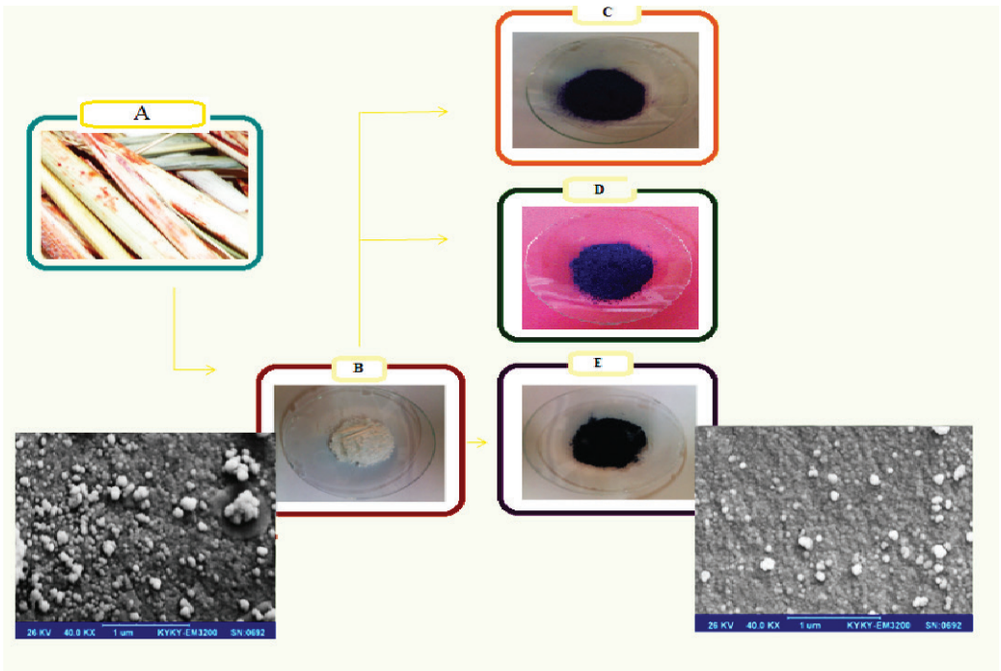

Fig. 1. Images for (A): stem sweep, (B): nanosilica extracted from stem sweep, and SEM micrograph of it, (C): CV adsorbed on nanosilica, (D): MB adsorbed on nanosilica, (E): CV and MB adsorbed on nanosilica, and SEM micrograph of it.

desired concentrations using distilled water to diminish the probable interferences. The solution pH values were measured using a Metrohm 744 pH-meter. The absorbance spectra for CV and MB were taken using a double-beam spectrophotometer (Rayleigh UV-2601) with a fixed slit width of 2 nm using a pair of quartz cells. The nanosilica functional groups were determined using an FT-IR spectrophotometer (WQF-520) in the scanning range of 4000–400 cm^{-1}. The X-ray diffraction pattern for nanosilica was recorded on an advance Bruker D8 X-ray diffractometer using Cu Kα radiation (28.5 mA, 35 KV) at λ = 1.5418 Å. A gas sorption system (Belsorp-Max, BEL, Japan Inc.) was used to determine the surface area and porosity property of the adsorbent. Also smoothing of the spectra was made using a Savitzky-Golly filter in the MATLAB software [19,20].

2.2. Dye adsorption studies

The dye adsorption experiments were carried out by addition of 50 mL of the dye solution with a definite initial concentration in the single and binary systems to a beaker containing a fixed amount of nanosilica at a given pH value. The solution was agitated under a constant stirring rate (400 rpm) at room temperature (30 ± 2°C). Then at the given time intervals 2, 6, 10, 15, 20, 30, 40, 50, 60, 70, and 80 min, 2 mL of the sample was withdrawn and centrifuged at 3400 rpm for 2 min to separate the solid and liquid phases. Subsequently, the residual dye concentration in the liquid phase was determined spectrophotometrically. The MB concentrations in the single and binary solution systems were determined using the calibration curve obtained by measuring the absorbance at the maximum wavelength (664 nm). For determination of the CV concentration in the binary solution, the first-order derivative of the spectral absorbance at the optimum wavelength (506 nm) was used. When the reaction reached the equilibrium, the individual removal percentage (R, %), and the adsorbed amount of each dye per unit weight of the adsorbent ($q_{e,i}$) were calculated using Eqs. (1) and (2), respectively [1].

$$R_i = \frac{\left(C_{0,i} - C_{e,i}\right)}{C_{0,i}} \times 100 \quad (1)$$

$$q_{e,i} = \frac{\left(C_{0,i} - C_{e,i}\right)V}{W} \quad (2)$$

where $C_{0,i}$ is the initial dye concentration (mg L^{-1}), $C_{e,i}$ is the residual dye concentration at equilibrium (mg L^{-1}), V is the solution volume (L), and W is the solid adsorbent mass (g).

2.3. Preparation of adsorbent

Nanosilica was extracted from stem sweep using the method reported by Kavian et al. [21]. In brief, stem sweep was firstly burned in air, and the black ash thus obtained was calcinated at 700°C to acquire a white ash, which was subsequently converted to sodium nanosilicate by refluxing it in NaOH solution (1 M) with vigorous stirring for 3 h. The resulting mixture was then filtered and neutralized with HCl solution (1 M) to obtain the gel form of silicic acid. After the polycondensation of this gel, it was filtered and washed with distilled water for several times, and then dried at 70°C overnight. Finally, it was ground using mortar and pestle to obtain a nanosilica powder (Fig. 1B). As a preliminary test, the capability of the prepared adsorbent for adsorption of CV and MB from their single and binary solution systems was approved by the change in the color of nanosilica after contacting with the studied dyes (Fig. 1.).

3. Results and discussion

3.1. Characterization

The powder XRD pattern for nanosilica is shown in Fig. 2. A well-resolved XRD pattern could be observed at 2θ of about 22°, which matched well with the reported pattern for nanosilica [21]. Also the N_2 adsorption-desorption isotherm for nanosilica is shown in Fig. 3. The sample exhibits a type IV isotherm with a characteristic H_2-hysteresis loop. According to the BJH method, the average pore diameter of nanosilica is 18.9 nm, indicating that it is a mesoporous material. The surface area of nanosilica, calculated using the Brunauer-Emmett-Teller (BET) equation, is 152 m^2 g^{-1} (Table 1).

In order to specify the functional groups responsible for the dye adsorption, the FT-IR spectra for the selected adsorbent were analyzed (Fig. 4). Before adsorption, the broad band at around 3462 cm^{-1} was assigned to the O-H stretching vibration of silanol or the water molecules trapped in nanosilica [22–25]. The very weak spectral band at 1650 cm^{-1} corresponds to the bending vibration of H-OH for the trapped water molecules in nanosilica matrix that could not be removed completely by heating [24]. The strong band at 1097 cm^{-1} and the relatively weaker bands at 800 cm^{-1} and 475 cm^{-1} refer to the asymmetric, stretching, and bending vibrations of Si-O-Si, respectively [22,24,25]. This spectrum was very similar to the FT-IR spectrum reported by the other researchers [24,25]. After loading the dyes on to the adsorbent, the O-H stretching and Si-O-Si asymmetric vibrations shifted to negative values along with reductions in the corresponding peak energies. These shifts and reductions in the band energies show that there is an interaction between the dye molecules and these functional groups [26–28].

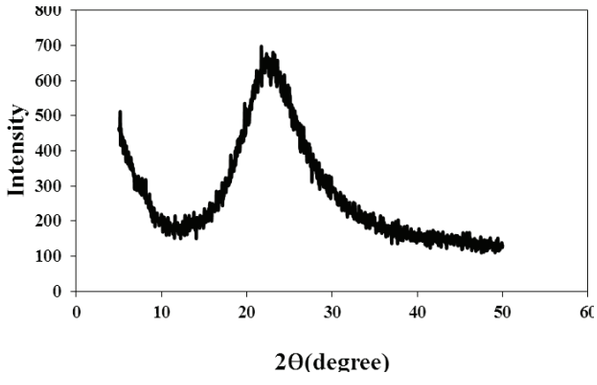

Fig. 2. XRD pattern for nanosilica.

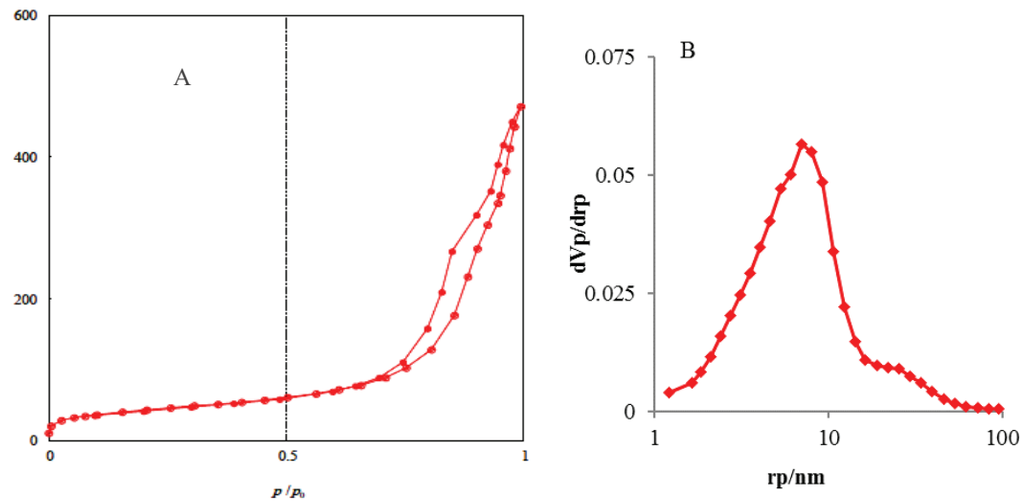

Fig. 3. N_2 adsorption–desorption isotherm (A) and corresponding BJH pore size distribution (B) of nanosilica.

Table1
Physico-chemical parameters of synthesized nanosilica

BET surface area ($m^2 g^{-1}$)	152
Total pore volume ($cm^3 g^{-1}$)	0.7193
Mean pore diameter (nm)	18.9
Micropore volume ($cm^3 g^{-1}$)	34.88

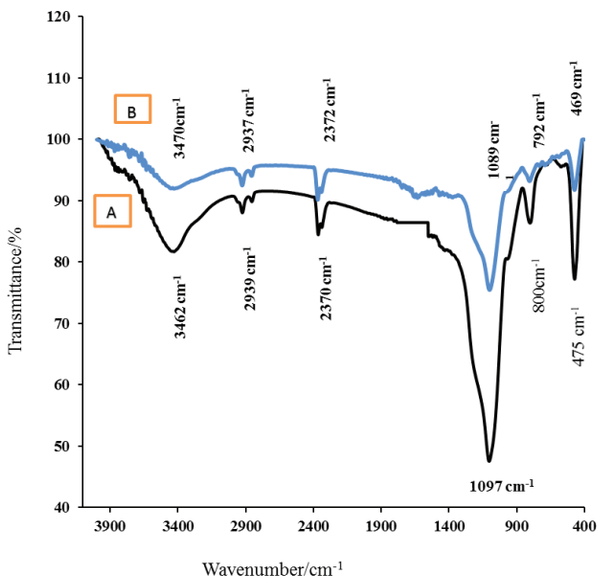

Fig. 4. FT-IR spectra for (A): pure and (B): dye-loaded adsorbent.

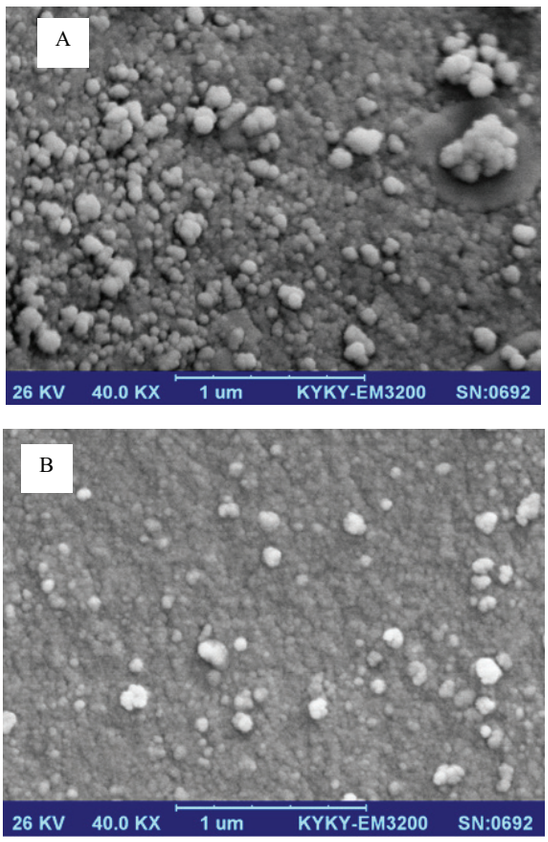

Fig. 5. SEM images for (A): pure nanosilica (B): dye-loaded nanosilica.

Also as it can be seen in the SEM image (Fig. 5B), after adsorption of the dyes, the surface of the dye-loaded nanosilica was smoother and homogenous than that for the unloaded nanosilica (Fig. 5A), which confirms the presence of the dye molecules on the adsorbent surface [29,30].

3.2. Simultaneous analysis of CV and MB in their binary mixture

The spectra recorded for the binary mixture of CV and MB with concentrations of 6 mg L^{-1} (Fig. 6) showed that

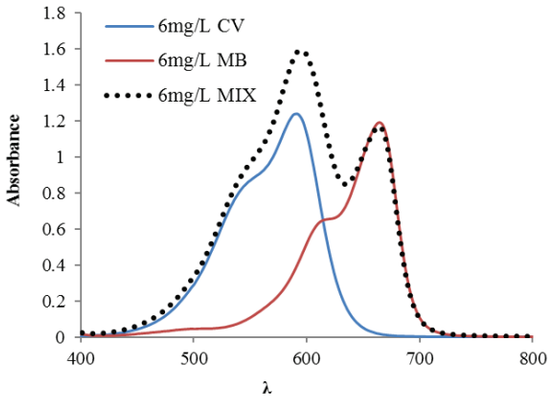

Fig. 6. Zero-order absorption spectra for CV and MB in single and binary systems.

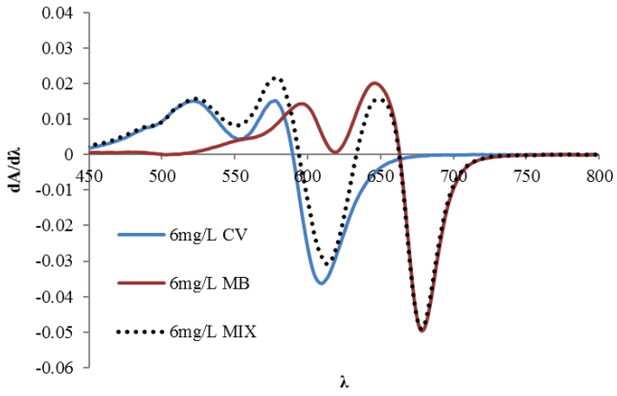

Fig. 7. First-order derivative absorption spectra for CV and MB in single and binary systems.

although in the maximum absorbance of MB there was no UV-visible spectral interference, the absorbance spectrum for CV overlapped with that for MB. This spectral overlapping led to a failure in the accurate determination of the CV dye in the binary mixture using the zero-order spectra. In order to overcome this problem, the derivative spectrophotometric method was used. According to the first-order derivative spectra for CV and MB in the single and binary systems (Fig. 7), CV could be determined at 506 nm (where absorbance of MB was zero). The calibration equation for CV was computed using its first-order signal at 506 nm *vs.* its different concentrations (Fig. 8). This equation was then used to determine the CV concentration in the binary solution.

In order to check the accuracy of the applied method to determine the content of the target compound content in the binary solution, different statistical parameters including the percent recovery and relative error (*E*, %) between the theoretical (C_t) and measured concentration (C_m) were computed using Eqns. (3) and (4), respectively, and the results obtained were tabulated in Table 2. The values obtained for these parameters showed that the proposed method could be successfully applied for the determination of the CV and MB contents in the mixture systems. Therefore, for the subsequent experiments, the absorbance spectra for the zero-order and first-order derivatives were used for determination of the MB and CV concentrations in the binary mixture, respectively.

$$Recovery = \frac{C_m}{C_t} \times 100 \quad (3)$$

$$Error(\%) = \frac{C_m - C_t}{C_t} \times 100 \quad (4)$$

3.3. Effect of pH

Since an adsorption process usually depends on the surface binding sites of the adsorbent and the chemistry of the dye [26,30], the solution pH was considered as a crucial parameter in the adsorption process [5]. Regarding this, in order to study the effect of this parameter and reveal its

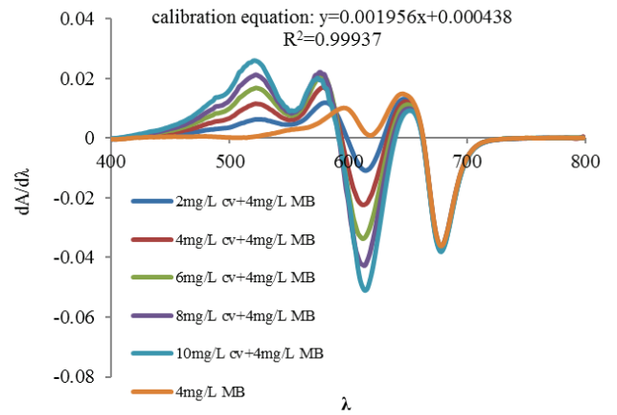

Fig. 8. First-order derivative absorption spectra for CV in binary solution in the range of 2–10 mg L^{-1} at constant MB concentration (4 mg L^{-1}).

optimum value, a definite amount of nanosilica (0.06 g) was added to 50 mL of the dye solutions (40 mg L^{-1}) at different pH values (from 3 to 10). A plot of the removal percentage as a function of pH is shown in Fig. 9. As it could be seen in this figure, the removal percentage of the dyes on nanosilica was remarkably promoted with enhancement in the pH value from 3.0 to 10. Similar observations have been accounted by other researchers for adsorption of these basic dyes [4,32–34]. This behavior can be explained based on the surface charge of the adsorbent and structure of the dyes. At lower pH values (in acidic solutions), protonation of silanol groups (due to a high H^+ concentration) causes an ionic repulsion between the protonated silanol and the cationic dyes. On the other hand, increasing the pH value leads to the presence of a negative charge on the adsorbent surface (due to deprotonation of silanol) [5]. Therefore, the electrostatic interaction between the positively charged sites of the dye molecules and negatively charged oxygen atoms of the adsorbent was enhanced, and finally, the removal percentage of the adsorbate was increased. This phenomenon was confirmed by shifting of the FT-IR spec-

Table 2
Percent recovery and relative error values for CV and MB in a binary mixture obtained by first- and zero-order derivative spectrophotometric methods, respectively

Theoretical mg L^{-1})		Measurement (mg L^{-1})		Recovery (%)		Error (%)	
C_{CV}	C_{MB}	C_{CV}	C_{MB}	C_{CV}	C_{MB}	*CV*	*MB*
9.50	3.00	9.66	3.18	101.68	106.00	1.68	6.00
3.00	3.00	2.96	2.93	98.71	97.66	–1.34	–2.29
0.00	5.00	–	5.02	–	100.42	–	0.42
5.00	5.00	4.83	4.84	96.60	96.80	3.37	–3.28
0.00	7.00	–	6.85	–	97.86	–	–2.19
7.00	7.00	7.08	6.93	101.14	99.02	1.17	–0.98
7.00	0.00	6.72	–	96.00	–	–4.00	–
9.00	9.00	9.20	8.67	102.22	96.33	2.22	–3.64
11.00	4. 50	11.12	4.37	101.09	97.12	1.09	–2.88
6.00	0.000	5.91	–	98.50	–	–1.50	–
12.00	15.00	12.01	14.90	100.83	99.33	0.083	–0.67

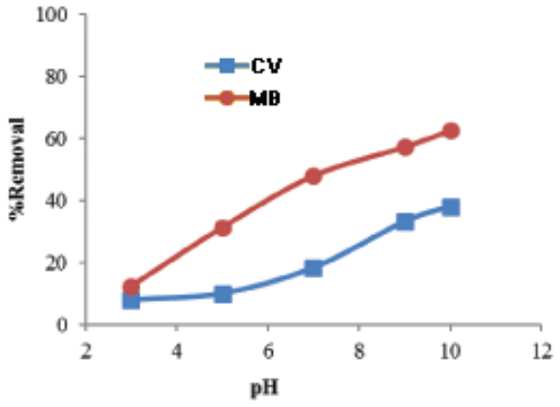

Fig. 9. Effect of solution pH on removal percentage of CV and MB by nanosilica (initial concentration = 40 mg L^{-1}; adsorbent dose = 0.04 g; temperature = 30 ± 2°C; contact time = 80 min).

trum after adsorption of the dyes (Fig. 4). Therefore, the following reactions probably take place at the adsorbent/adsorbate interface [4, 5]:

$$SiOH + H^+ \rightarrow SiOH_2^+$$

$$SiOH_2^+ + dye^+ \rightarrow SiOH_2^+ \leftrightarrow dye^+ \quad \text{(electrostatic repulsion in acidic solutions)}$$

$$SiOH + OH^- \rightarrow SiO^- + H_2O$$

$$SiO^- + dye^+ \rightarrow SiO^- \ldots . dye^+ \quad \text{(electrostatic interaction in alkaline solutions)}$$

Thus the optimum pH value for the subsequent experiments was selected to be 10, in which maximum removal occurred for both dyes.

The results of the study performed also showed that pH alone had no effect on the percentage dye removal.

3.4. Effect of adsorbent dosage

In this part of the work, the effect of different nanosilica dosage (0.06–0.12 g) on the adsorption of CV and MB was studied in the range of 20–100 mg L^{-1} at the optimum pH value. The plots of removal percentage *vs.* adsorbent dosage for both dyes are presented in Fig. 10. As one could see in this figure, the removal percentage augmented with increase in the adsorbent dosage. This phenomenon can be explained by the increase in the surface area of the adsorbent and active adsorption sites in nanosilica as the adsorbent dosage is increased [9,11].

3.5. Effect of contact time and initial dye concentration

In order to design economical wastewater treatment systems, the equilibrium time is recognized as one of the most important factors. Therfore, the removal of CV and MB in the range of 20–100 mg L^{-1} versus contact time was surveyed to speceify the adsorption equilibrium time. The results obtained (Fig. 11) showed that adsorption of the dyes onto nanosilica took place at a high rate in the first 10 min for all the initial dye concentrations. After this stage, the adsorption rate decreased slowly, and finally, it came into the equlibrim in 50–80 min for all the studied concentrations. The rapid uptake in the early times can be attributed to the high concentration gradient and availabilty of the unoccupied sites [35,36]. Also in order to study the effect of the initial dye concetration on the removal percentage, different amounts of nanosilica (from 0.06 to 0.12 g) were added to 50 mL of the solution at the concentrations of 20, 40, 60, 80, and 100 mg L^{-1}; pH 10; and contact times of 2–80 min. According to the results obtained (Fig. 12), it should be stressed that the removal percentage (R_i) decreases with increase in the initial concentration. This observation can be explained based on the ratio of the accessible active sites of the adsorbent to the dye moles [36]. This ratio was high at low concentrations, while at a high initial concentration, it became less, and thus R_i decreased.

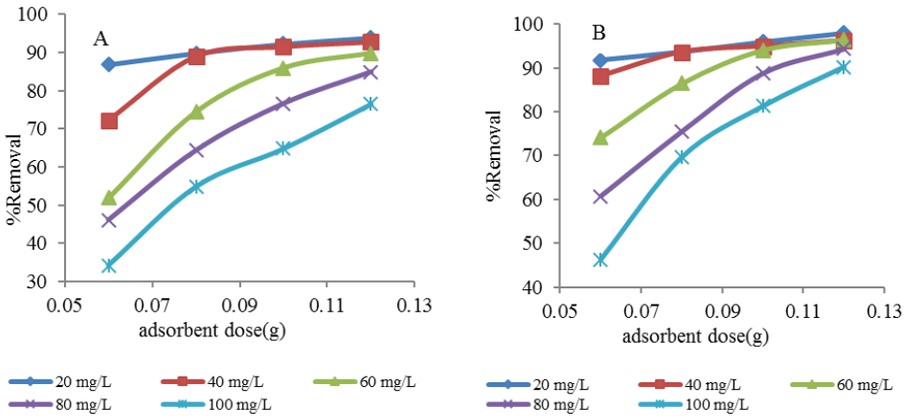

Fig. 10. Effect of adsorbent dosage on removal percentage of dyes at different concentrations of (A): CV and (B): MB.

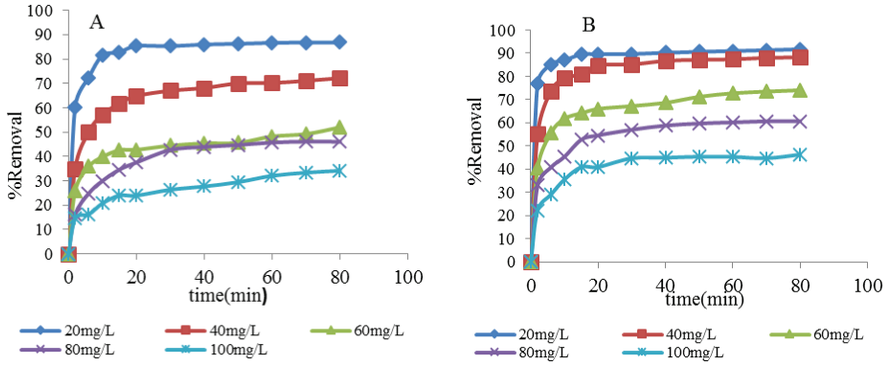

Fig. 11. Effect of contact time on removal percentage of dyes at different concentrations of (A) CV and (B) MB.

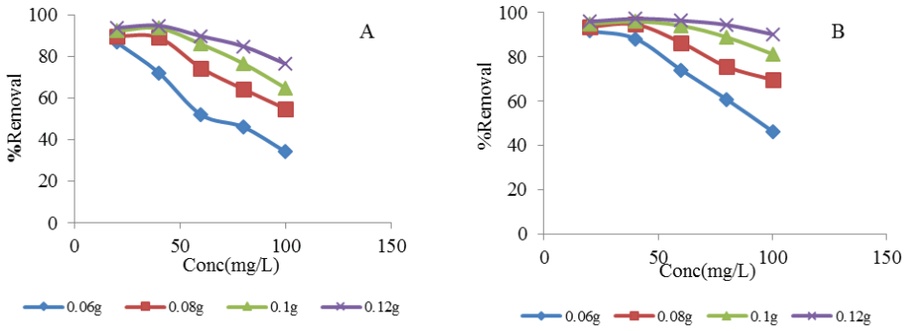

Fig. 12. Effect of initial concentration on removal percentage of dyes at different adsorbent dosages for (A) CV and (B) MB.

3.6. Studying adsorption isotherm

A successful application of the adsorption technique demands studies based on various adsorption isotherms [37]. An adsorption isotherm is basically important to describe the relationship between the amount of adsorbate uptaken by the adsorbent and the adsorbate concentration remaining in the solution.

There are different isotherms available to describe the equilibrium data for the process of adsorption onto a solid surface. In this work, two well-known isotherms, the Freundlich and the Langmuir isotherms, were appllied to evaluate the sorption of dyes at various initial concentrations (ranging from 20 to 100 mg L^{-1}) on a constant amount of nanosilica (0.1 g). The Langmuir model is based upon

a monolayer coverage of adsorbate on the adsorbent surface that is energetically homogenous. This isotherm can be defined as follows [38]:

$$q_e = k_f c_e^{\frac{1}{n}} \tag{6}$$

where q_{eq}, q_{max}, k_l, and c_e are the equilibrium dye uptake (mg g^{-1}), theoretical maximum adsorption capacity (mg g^{-1}), Langmuir constant (L mg^{-1}), and equilibrium concentration (mg L^{-1}), respectively.

The Freundlich model assumes that adsorption occurs on a heterogeneous surface or sites having different affinities [38,39].

$$RMSE = \sqrt{\frac{\Sigma(q_{e,\exp} - q_{e,cal})^2}{N}} \tag{6}$$

where the parameters k_f, C_e, and n are indicative of the relative sorption capacity ((mg g^{-1}) (L $mg^{-1})^{1/n}$), equilibrium concentration of the dye in the bulk solution (mg L^{-1}), and sorption intensity, respectively [39].

The isotherm constants for each isotherm for both dyes in a single solution (see Table 3) were obtained by the non-linear regression using the Matlab software (version 2013b). In this method, the statistical parameters of the root mean square error (RMSE) and correlation coefficient (R^2), defined as below, were applied for estimating the prediction accuracy and the extent of agreement between the experimental results and the results predicted by each model. The model having the lowest RMSE value and largest R^2 value was selected as the appropriate model.

$$RMSE = \sqrt{\frac{\Sigma(q_{e,\exp} - q_{e,cal})^2}{N}} \tag{7}$$

$$R^2 = 1 - \frac{\Sigma\left(q_{e,\exp} - q_{\exp,cal}\right)^2}{(q_{e,\exp} - \overline{q}_{e,\exp})^2} \tag{8}$$

According to Table 3, one can conclude that the Langmuir isotherm is more suitable for the interpretation of the experimental data over the full concentration range. This manner was observed for the adsorption of MB onto nanosilica extratced from diatomaceous earth, and the adsorption of MB onto commerical silica [16,40].

In addition, the favorable nature of adsorption can be evaluated in terms of the separation factor (R_L) [41 ,42]:

$$R_L = \frac{1}{1 + k_l c_0} \tag{9}$$

where k_l is the Langmuir constant and c_0 is the highest initial concetration of the adsorbate present in the solution. The values obtained for this parameter (Table 3), which were less than 1 and greater than zero, emphasized that the adsorption process was favorable for both dyes [7,42]. Also based on q_{max} for the other adsorbents tabulated in Table 4, the proposed adsorbent displays a comparable performance, and can have potential applications for purification of effluents having these dye classes.

In continuation, the Sheindorf-Rebuhn-Sheintuch model (as a Freundlich-type isotherm) [30] and the extended Langmuir model [6], defined by Eqs. (10) and (11), respectively, were applied to describe the adsorption behavior in the binary mixture.

$$q_{e,,i}^{j} = k_{f,i} c_{e,i} (c_{e,i} + \theta_{ij} c_{e,j})^{\left(\frac{1}{n_i} - 1\right)} \tag{10}$$

Table 3
Parameter values for single component isotherms computed by non-linear least squares method

Isotherms	Parameters	Dye	
		CV	MB
Freundlich	k_f	15.13	17.09
	n	2.94	3.17
	R^2	0.9071	0.9031
	RMSE	3.26	3.42
Langmuir	q_{max}	45.71	44.81
	k_L	0.34	0.49
	R_L	0.028	0.020
	R^2	0.9833	0.9930
	RMSE	1.39	0.92

Table 4
Comparison between maximum adsorption capacities of various reported adsorbents computed using Langmuir isotherm for removal of CV and MB

Adsorbent	Adsorbate	Adsorption Capacity (mg/g)	Ref.
Amourph silica	MB	22.0	[16]
Silica (from spent diatomaceous)	MB	56.20	[40]
Casuarina equisetifolia needle	MB	110.8	[43]
Peat of Brunei Darussalam	MB	111	[44]
Functionalized silica nanoparticles	MB	500	[45]
Ashoka (Saraca asoca) leaf powder	MB	90.9	[46]
Fly ash	MB	5.60	[47]
Posidonia oceanica (L.) dead leaves	MB	217.39	[48]
Nanosilica (from stem sweep)	MB	44.81	Present work
Soil	CV	20	[49]
$CaFe_2O_4$	CV	0.87	[50]
Coal	CV	6.25	[51]
Coniferous pinus bark powder	CV	32.78	[52]
Magnetic tea waste	CV	113.64	[53]
Nanosilica (from stem sweep)	CV	45.71	Present work

$$q_{eq,j} = \frac{q_{\max,j} k_{l,j} c_{e,j}}{1 + \sum_{j=1}^{2} k_{l,j} c_{e,j}} \quad (11)$$

In these equations, $k_{f,i}$ and n_i are the Freundlich isotherm constants acquired for both dyes from the corresponding single-component isotherm, q_{ij} is the competition coefficient that illustrates the inhibition for the adsorption of component '*i*' by component '*j*', which is estimated by non-linear fitting, and $q_{e,i}{}^{j}$ and c_e are the adsorbed amount of component '*i*' in the presence of component '*j*' and equilibrium concentration, respectively. In the extended Langmuir isotherm, the constants $q_{max,j}$ and $k_{l,j}$ are the maximum adsorption capacity (mg g^{-1}) and Langmuir constant (L mg^{-1}) for component '*j*', respectively, obtained via a non-linear analysis employing the Matlab software (Table 5). The results obtained obviously display that the extended Langmuir isotherm can describe the equilibrium data in the binary mixture. Also based on Table 5, the existence of other dyes reduces the q_{max} and k_l values. The decrease in the values for these parameters by the secondary copollutant presumably reflects the antagonistic interaction between the dyes for binding on the sites [30]. The reduction percentage of q_{max} can be computed by Eq. (12).

$$Reduction(\%) = \frac{(q_{\max,single} - q_{\max,binary)}}{q_{\max,single}} \times 100 \quad (12)$$

The values of this parameter for the CV and MB dyes were 36.2 and 13.10%, respectively. Due to a more stabilized positive charge at the sulfur atom in the structure of MB [5], the interaction between this atom and the negatively charged oxygen atom in nanosilica is stronger than the interaction between the positively charged nitrogen atom in the structure of CV and the adsorbent surface. Consequently, the selected adsorbent has a higher affinity (k_l) toward MB with respect to CV. These results are similar to those reported by Kurniawan et al. [5] for the simultaneous adsorption of malachite green and MB onto bentonite (containing a high amount of silica).

Table 5
Values for multi-component isotherm parameters in a binary system

Isotherms	Parameters	Dye	
		CV	MB
Sheindorf-Rebuhn	θ_{ij}	2.45	0.416
	R^2	0.9186	0.8771
	RMSE	1.77	3.08
Extended Langmuir	q_{max}	29.16	38.94
	$k_{l,1}$	0.272	0.355
	$k_{l,2}$	0.0080	0.013
	R^2	0.9709	0.9532
	RMSE	1.07	1.90

3.7. Adsorption kinetic study

In order to determine the time neccessary to reach the equilibrium, and to clarify the mechanism and the adsorption rate, which is essential for the design of sorption industrial columns [41], the adsorption kinetics should be investigated. For this purpose, the concentration changes as a function of time were measured, and the two most frequently used kinetic models (pseudo-first and pseudo-second order models) were applied to simulate the experimental data. The equations involved are defined as follow [6,14,17]:

$$\ln(q_e - q_1) = \ln(q_e) - k_1 t \quad (13)$$

$$\frac{t}{q_t} = \frac{1}{k_2 q_e^2} + \frac{1}{q_{eq}} t \quad (14)$$

where the parameters q_e and q_t (mg g^{-1}) are the adsorbed amount of the dye at equilibrium and time t (min), respectively, and k_1 (min^{-1}) and k_2 (g mg^{-1} min^{-1}) are the corresponding rate constants of adsorption. For the pseudo-first order kinetics model, the constansts k_1 and q_e are obtained using the slope and intercept of the plot of $\ln(q_e - q_t)$ *vs.* t, while for the second-order kinetics model, the constants k_2 and q_e are obtained using the intercept and slope of the plot of (t/q_t) *vs.* t, respectively. The value for q_e, acquired from the corresponding plots, is named as the calculated q_e (or $q_{e,cal}$). Based on the results obtained (Table 6), the values for this parameter, calculated by the second-order kinetics model, are much closer to the experimental ones with respect to the values calculated by the first-order kinetics model for all the initial dye concentrations in the single and binary systems. In addition, the R^2 values for this model were higher when compared with the corresponding values in the first-order kinetics model. Based on these observations, the adsorption reaction of the dyes well-fitted to the second-order kinetics model over the whole time range in the single and binary systems. Similar results were obtained for the adsorption of MB onto silica extracted from diatomaceous [40].

3.8. Modeling

3.8.1. Modeling simultanous removal of CV and MB in binary solution by random forest model

The random forest (RF) model is a classification and regression method, and consists of a collection of the decision trees used collectively to determine the desired output [54]. Each tree is constructed from a bootstrap sample drawn with replacement from the original dataset, and the prediction is done by majority vote (in classification) or via averaging (in regression) [55,56]. In each bootstrap sample, the data was randomly split into the in-bag data (for training the RF model) and out of bag (OOB) data (for evaluation of the prediction error of model).

This algorithm has three adjustable parameters: the number of regression trees (ntree),the number of input variables or predictors to try at each node in each tree (mtry), and the minimum size of terminal nodes in each tree (node size) [18,55].

Table 6
Kinetic parameters for adsorption of dyes onto prepared adsorbent in single solution and binary mixture

System	Dye	Pseudo-first-order				Pseudo-second-order		
		$q_{e\,(exp.)}$	$q_{e\,(cal.)}$	k_1	R^2	$q_{e\,(cal.)}$	k_2	R^2
Single	CV							
	40	19.86	4.89	0.0800	0.8382	20.12	0.0550	0.9999
	60	26.5	12.21	0.0692	0.9366	27.32	0.0110	0.9997
	80	35.50	18.34	0.0631	0.9403	36.90	0.008	0.9997
	100	38.95	23.44	0.0616	0.9886	41.32	0.005	0.9986
	MB							
	40	19.69	2.58	0.095	0.9345	19.84	0.10	1.000
	60	28.94	13.79	0.069	0.9795	29.67	0.014	0.9995
	80	36.11	21.69	0.067	0.9607	37.73	0.009	0.9993
	100	39.82	29.52	0.052	0.9710	41.32	0.0062	0.9976
	CV							
	40	17.91	5.34	0.066	0.8256	18.28	0.033	0.9997
Binary	60	22.54	14.89	0.052	0.9752	23.87	0.007	0.9969
	80	25.38	18.74	0.043	0.9589	27.25	0.0044	0.9940
	100	26.71	21.00	0.04	0.9610	29.15	0.0029	0.9922
	MB							
	40	20.28	5.29	0.096	0.9255	20.49	0.064	1.000
	60	25.91	14.00	0.067	0.9754	26.81	0.0010	0.9995
	80	31.72	17.55	0.053	0.9470	32.79	0.0080	0.9989
	100	34.79	19.63	0.064	0.9419	36.76	0.0050	0.9985

The steps involved in the execution of an RF regression model can be described as below:

(i): Using the bootstrapping method, the dataset was split into in-bag samples (2/3 of data) and the OOB sample (1/3 of data). (ii): Decision trees were constructed using the in-bag samples, and at each node of them a small random subset of variables (mtry) were selected instead of using all the input variables. (iii): The node size variable was initialized, and a regression model based on the ntree, mtry, and node size variables was created. (iv): Estimation of the output was made using each tree for all of the samples in the OOB series, and their average was considered as the final predicted output for each data existing in OOB. (v) The performance of the constructed model was estimated by calculating MSE for the OOB series.

These steps were reiterated, and the optimal values for the ntree, mtry, and node size variables were selected by minimizing MSE for the OOB subset.

Thus for the implementation of the RF model, the experimental data was randomly divided into the training subset (75%) and testing subset (25%). The input variables (predictors) to the RF were the initial concentration (20, 40, 60, 80, and 100 mg/L), adsorbent dosage (0.06, 0.08, 0.10, and 0.12 g), and contact time (2–80 min). The output variable was the removal percentage. Then at different values for the node size (from 2 to 9), the values for n_{tree} and m_{try} changed simultaneously, ranging from 25 to 500 (with a step size of 25) and from 2 to 3 (with a step size of 1.0), respectively, and the criterion in the optimization of the mentioned factors was minimization of RMSE of the OOB samples. The respective OOB RMSE at a constant value of node size = 2 and different values of ntree and mtry are shown in Fig. 13. According to these figures, for CV at ntree = 200 and mtry = 2, RMSE of the OOB data is minimized (Fig. 13A), while for MB, at ntree = 175 and mtry = 2, RMSE of the OOB data is minimized (Fig. 13B).

3.8.2. Modeling simulatanous removal of CV and MB in binary solution by Multiple linear regression

One of the earliest methods used for modeling is the multiple linear regression (MLR). The simplicity, transparency, and easy interpretability are recognized as the most important advantages of this method [57]. The generalized expression applied for it is as follows:

$$y = b_0 + b_1 x + b_2 x + \ldots + b_n x_n \tag{15}$$

where b_0 and b_i (i = 1,…,n) are the intercept and regression coefficients, respectively, determined using the least squares method.

To check whether there is a linear relationship between the predictor variables and the removal percentage, the MLR model was generated by a training set with three experimental factors as the independent variables:

Removal percentage of CV = 0.769 – 0.880Concentration + 0.148Adsorbent dose + 0.128Contact time (16)

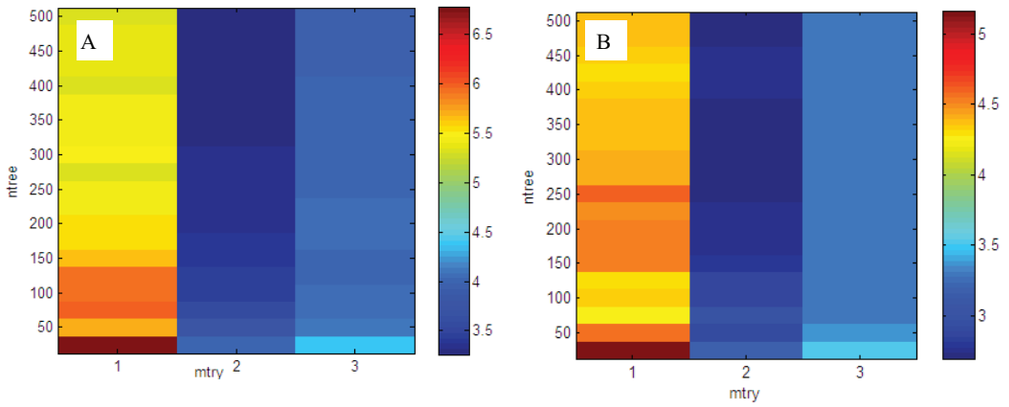

Fig. 13. RMSEs of OOB data at node size = 2 and different values of ntree and mtry for (A): CV and (B): MB.

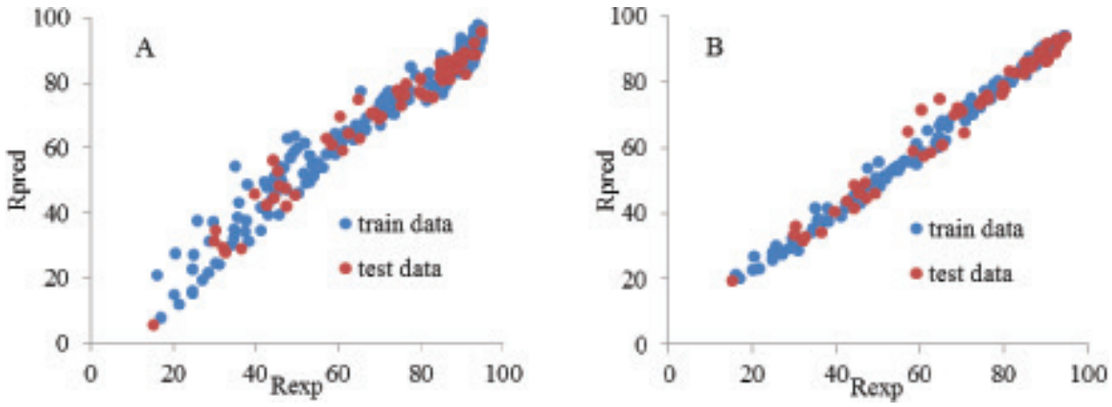

Fig. 14. Plot of predicted against experimental removal percentage values of CV for training set and test set by (A): MLR and (B): RF method.

Removal percentage of MB = 0.843 – 0.907Concentration + 0.109Adsorbent dose + 0.088Contact time (17)

These linear models were used to foretell the removal percentage of samples in the external test.

3.8.3. Evaluation of constructed models by RF and MLR methods

Ideally, an assessment of the performance of a predictive model should be made using a large independent test dataset that is not present in the training process [58]. For this purpose, the developed MLR and RF models were employed to estimate the removal percentage of 55 samples in the external set. The respective results are demonstrated in Fig. 14. Different statistical parameters such as RMSE, mean relative error (MRE), and R^2, defined by Eqns. (18)–(20), respectively [55], were used to examine the prediction accuracy.

$$MRE = \frac{\sum_{i=1}^{N}\left|\frac{(y_i - y_i)}{y_i}\right|}{N} \times 100 \quad (18)$$

$$RMSE = \sqrt{\frac{\Sigma(y_i - y_i)^2}{N}} \quad (19)$$

where y_i is the experimental removal percentage value for sample i, $\hat{y}_i$ is the predicted value for sample i, $\overline{y}$ is the mean experimental removal percentage value, and N is the number of samples in the understudied set. Based on the values for these parameters (Tables 7 and 8), a comparison between the MLR and RF models confirms that the RF model has a substantially better and more accurate prediction with respect to the MLR one.

3.9. Regeneration of proposed adsorbent

A suitable adsorbent should not only have high adsorption capacities but also show excellent regeneration characteristics to make the adsorption process cost-effective [59]. Thus to test the probability of recycling the nanosilica beads, distilled water (50 mL) was added to exhausted nanosilica (1.00 g). Then a few drops of a dish-washing liquid were added to the mixture, which was stirred for 30 min. After

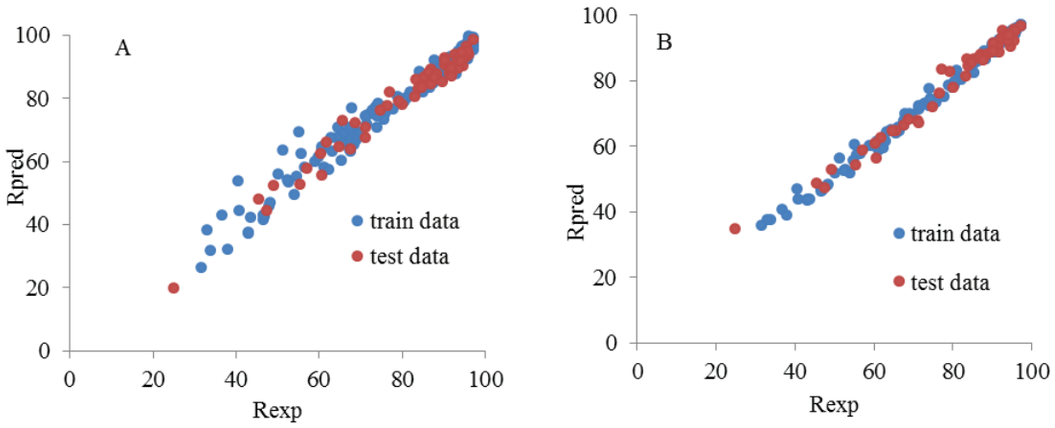

Fig. 15. Plot of predicted against experimental removal percentage values of MB for training set and test set (A): MLR and (B): RF method.

Table 7
Statistical parameters for evaluation of accuracy of constructed MLR and RF models for CV

Parameter	MLR		RF	
	Training	Test set	Training	Test set
MRE	8.10	6.74	2.77	4.36
RMSE	2.69	4.44	1.80	3.29
R^2	0.9506	0.9540	0.9944	0.9754

Table 8
Statistical parameters for evaluation of accuracy of constructed MLR and RF models for MB

Parameter	MLR		RF	
	Training	Test set	Training	Test set
MRE	3.68	3.17	1.47	2.69
RMSE	1.50	2.68	1.41	2.41
R^2	0.9650	0.9711	0.9943	0.9781

that, the adsorbent was washed three times with distilled water. Then 0.10 g of the oven-dried adsorbent was used for the removal of 50 mL of 40 ppm of the dye in the binary mixture. The results obtained revealed that the efficiency of the regenerated nanosilica was constant at 90% at 4 cycles of the adsorption process.

4. Conclusions

In the present work, for the first time, nanosilica (extracted from stem sweep) was used for the removal of dyes. With respect to other agricultural wastes such as rice husk, applied for the removal of dyes, stem sweep has few reported useful applications, and due to its hardness, it cannot be used as food for birds and animals. Consequently, it is appropriate to be replaced as an inexpensive adsorbent. Investigation of the experimental data revealed that (i) adsorption of CV and MB onto nanosilica depended severely on the experimental conditions including the solution pH, adsorbent dosage, contact time, and initial dye concentration; (ii) the prepared sorbent demonstrated a higher affinity toward MB than CV in a binary mixture; (iii) the adsorption kinetics of these dyes followed a pseudo-second order kinetics; (iv) the Langmuir isotherm described the equilibrium data logically. Also the results obtained from the RF model implied that the it could forecast the removal percentage values with a better accuracy than the MLR model. Therefore, this method is useful for the development of an automated wastewater dye removal plant.

Acknowledgment

The authors are thankful to the Shahrood University of Technology Research Council for the support of this work.

References

[1] J.F. Gao, Q. Zhang, K. Su, J.H. Wang, Competitive biosorption of Yellow 2G and Reactive Brilliant Red K-2G onto inactive aerobic granules: Simultaneous determination of two dyes by first-order derivative spectrophotometry and isotherm studies, Bioresour. Technol., 101(2010) 5793–5801.
[2] Y. Xi, Y. F. Shen, F. Yang, G. J. Yang, C. Liu, Z. Zhang, Removal of azo dye from aqueous solution by a new biosorbent prepared with Aspergillus nidulans cultured in tobacco wastewater, J. Taiwan Inst. Chem. Eng., 44 (2013) 815–820.
[3] S. Hajati, M. Ghaedi, B. Barazesh, F. Karimi, R. Sahraei, A. Daneshfar, A. Asghari, Application of high order derivative spectrophotometry to resolve the spectra overlap between BG and MB for the simultaneous determination of them: Ruthenium nanoparticle loaded activated carbon as adsorbent, J. Ind. Eng. Chem., 20 (2014) 2421–2427.
[4] T.S. Anirudhan, M. Ramachandran, Adsorptive removal of basic dyes from aqueous solutions by surfactant modified bentonite clay (organoclay): Kinetic and competitive adsorption isotherm, Process Saf. Environ. Prot., 95 (2015) 215–225.

[5] A. Kurniawan, H. Sutiono, N. Indraswati, S. Ismadji, Removal of basic dyes in binary system by adsorption using rarasaponin–bentonite: Revisited of extended Langmuir model, Chem. Eng. J., 89–190 (2012) 264–274.
[6] D. Shen, J. Fan, W. Zhou, B. Gao, Q. Yue, Q. Kang, Adsorption kinetics and isotherm of anionic dyes onto organo-bentonite from single and multisolute systems, J. Hazard Mater., 172 (2009) 99–107.
[7] G.O. El-Sayed, Removal of methylene blue and crystal violet from aqueous solutions by palm kernel fiber, Desalination, 272 (2011) 225–232.
[8] M.C. Somasekhara Reddy, V. Nirmala. Bengal gram seed husk as an adsorbent for the removal of dyes from aqueous solutions – Equilibrium studies, Arab. J. Chem., [volume??] (2014) [pages??]
[9] M. Anbia, S.A. Hariri, S.N. Ashrafizadeh, Adsorptive removal of anionic dyes by modified nanoporous silica SBA-3, Appl. Surf. Sci., 256 (2010) 3228–3233.
[10] R.K. Gautam, A. Mudhoo, M.C. Chattopadhyaya, Kinetic, equilibrium, thermodynamic studies and spectroscopic analysis of Alizarin Red S removal by mustard husk, J. Environ. Chem. Eng., 1 (2013) 1283–1291.
[11] M. Ghaedi, S. Hajati, B. Barazesh, F. Karimi, G. Ghezelbash, Saccharomyces cerevisiae for the biosorption of basic dyes from binary component systems and the high order derivative spectrophotometric method for simultaneous analysis of Brilliant green and Methylene blue, J. Ind. Eng. Chem., 19 (2013) 227–233.
[12] M. Arshadi, A.R. Faraji, M.J. Amiri, M. Mehravar, A. Gil, Removal of methyl orange on modified ostrich bone waste – A novel organic–inorganic biocomposite, J. Colloid Interface Sci., 446 (2015) 11–23.
13] N. Priyantha, L.B.L. Lim, M.K. Dahri, Dragon fruit skin as potential biosorbent for the removal of methylene blue dye from aqueous solution, Int. Food Res. J., 22 (2015) 2141–2148.
[14] L.B.L. Lim, N. Priyantha, H.I. Chieng, M.K. Dahri, Artocarpus camansi Blanco (Breadnut) core as low-cost adsorbent for the removal of methylene blue: equilibrium, thermodynamics and kinetics studies, Desal. Water Treat., 57 (2016) 5673–5685.
[15] H.I. Chieng, L.B.L. Lim, N. Priyantha, Enhancement of crystal violet adsorption on Artocarpus camansi peel through sodium hydroxide treatment, Desal. Water Treat., 58 (2017) 320–331.
[16] C.D. Woolard, J. Strong, C.R. Erasmus, Evaluation of the use of modified coal ash as a potential sorbent for organic waste streams, Appl. Geochem., 17 (2002) 1159–1164.
[17] M. Ghaedi, A. Ansari, F. Bahari, A.M. Ghaedi, A. Vafaei, Hybrid artificial neural network and particle swarm optimization for prediction of removal of hazardous dye brilliant green from aqueous solution using zinc sulfide nanoparticle loaded on activated carbon, Spectrochim. Acta Part A Mol. Biomol. Spectrosc., 137 (2015) 1004–1015.
[18] F. Heydari, M. Ghaedi, A. Ansari, M.A. Ghaedi, Random forest model for removal of methylene blue and lead (II) ion using activated carbon obtained from tamarisk, Desal. Water Treat., 57 (2016) 19273–19291.
[19] S. Hajati, S. Tougaard, J. Walton, N. Fairley, Noise reduction procedures applied to XPS imaging of depth distribution of atoms on the nanoscale, Surface Sci., 602 (2008) 3064–3070.
[20] S. Hajati, S. Coultas, C. Blomfield, S. Tougaard, Nondestructive quantitative XPS imaging of depth distribution of atoms on the nanoscale, Surf. Interf. Analysis, 40 (2008) 688–691.
[21] S. Kavian, S.N. Azizi, S. Ghasemi, Fabrication of novel nanozeolite-supported bimetallic Pt Cu nanoparticles modified carbon paste electrode for electrocatalytic oxidation of formaldehyde, Int. J. Hydrogen Energy, 41(2016) 14026–14035.
[22] U. Kalapathy, A. Proctor, J. Shultz, A simple method for production of pure silica from rice hull ash, Bioresour. Technol., 73 (2000) 257–262.
[23] S. Hu, Y.L. Hsieh, Preparation of activated carbon and silica particles from rice straw, ACS Sustain. Chem. Eng., 2 (2014) 726–734.
[24] M.A. Rida, F. Harb, Synthesis and characterization of amorphous silica nanoparitcles from aqueous silicates using cationic surfactants, J. Metals Mater. Miner., 24 (2014) 37–42.
[25] K. Srivastava, N. Shringi, V. Devra, A. Rani, Pure silica extraction from perlite: Its characterization and affecting factors. Int. J. Innov. Res. Sci. Eng. Technol., 2 (2013) 2936–2942.
[26] T. Akar, I. Tosun, Z. Kaynak, E. Ozkara, O. Yeni, E.N. Sahin, S.T. Akar, An attractive agro-industrial by-product in environmental cleanup: Dye biosorption potential of untreated olive pomace, J. Hazard. Mater., 166 (2009) 1217–1225.
[27] A. Gürses, A. Hassani, M. Kıranşan, O. Açışlı, S. Karaca, Removal of methylene blue from aqueous solution using by untreated lignite as potential low-cost adsorbent: Kinetic, thermodynamic and equilibrium approach, J. Water Process Eng., 2 (2014) 10–21.
[28] R. Lafi, A. Ben Fradj, A. Hafiane, B. Hameed, Coffee waste as potential adsorbent for the removal of basic dyes from aqueous solution, Korean J. Chem. Eng., 31 (2014) 2198–2206.
[29] S. Chowdhury, R. Mishra, P. Saha, P. Kushwaha, Adsorption thermodynamics, kinetics and isosteric heat of adsorption of malachite green onto chemically modified rice husk, Desalination, 265 (2011) 159–168.
[30] M. Turabık, B. Gozmen, Removal of basic textile dyes in single and multi-dye solutions by adsorption: statistical optimization and equilibrium isotherm studies, CLEAN–Soil, Air, Water, 41 (2013) 1080–1092.
[31] M. Ghaedi, H. Hossainian, M. Montazerozohori, A. Shokrollahi, F. Shojaipour, M. Soylak, M. Purkait, A novel acorn based adsorbent for the removal of brilliant green, Desalination, 281 (2011) 226–233.
[32] X.S. Wang, X. Liu, L. Wen, Y. Zhou, Y. Jiang, Z. Li, Comparison of basic dye crystal violet removal from aqueous solution by low-cost biosorbents, Sep. Sci. Technol., 43 (2008) 3712–3731.
[33] S. Chakraborty, S. Chowdhury, P.D. Saha, Adsorption of crystal violet from aqueous solution onto NaOH-modified rice husk, Carbohydr. Polym., 86 (2011) 1533–1541.
[34] M. Peydayesh, A. Rahbar-Kelishami, Adsorption of methylene blue onto Platanus orientalis leaf powder: Kinetic, equilibrium and thermodynamic studies, J. Ind. Eng. Chem., 21 (2015) 1014–1019.
[35] S. Banerjee, G.C. Sharma, R.K. Gautam, M.C. Chattopadhyaya, S.N. Upadhyay, Y.C. Sharma, Removal of Malachite Green, a hazardous dye from aqueous solutions using Avena sativa (oat) hull as a potential adsorbent, J. Mol. Liq., 213 (2016) 162–172.
[36] N.M. Mahmoodi, R. Salehi, M. Arami, Binary system dye removal from colored textile wastewater using activated carbon: Kinetic and isotherm studies, Desalination, 272 (2011) 187–195.
[37] A. Shokrollahi, A. Alizadeh, Z. Malekhosseini, M. Ranjbar, Removal of bromocresol green from aqueous solution via adsorption on ziziphus nummularia as a new, natural, and low-cost adsorbent: kinetic and thermodynamic study of removal process, J. Chem. Eng. Data., 56 (2011) 3738–3746.
[38] M. Turabik, Adsorption of basic dyes from single and binary component systems onto bentonite: Simultaneous analysis of Basic Red 46 and Basic Yellow 28 by first order derivative spectrophotometric analysis method, J. Hazard. Mater., 158 (2008) 52–64.
[39] S. Elemen, E.P. Kumbasar, S. Yapar, Modeling the adsorption of textile dye on organoclay using an artificial neural network, Dyes Pigm., 95 (2012) 102–111.
[40] W. Tsai, K. Hsien, J. Yang, Silica adsorbent prepared from spent diatomaceous earth and its application to removal of dye from aqueous solution, J. Colloid Interface Sci., 275 (2004) 428–433.
[41] K.V. Kumar, A. Kumaran, Removal of methylene blue by mango seed kernel powder, Biochem. Eng. J., 27 (2005) 83–93.
[42] M.A. Ahmad, N. Ahmad, O.S. Bello, Modified durian seed as adsorbent for the removal of methyl red dye from aqueous solutions, Appl. Water Sci., 5 (2015) 407–423.
[43] L.B.L. Lim, N. Priyantha, C.H. Ing, C. Bandara, Sorption characteristics of peat of Brunei Darussalam I: Preliminary characterization and equilibrium studies of methylene blue - peat interactions, Ceylon J. Sci. (Phys. Sci.), 17 (2013) 41–51.

[44] M.K. Dahri, M.R. Rahimi Kooh, L.B.L. Lim, Application of Casuarina equisetifolia needle for the removal of methylene blue and malachite green dyes from aqueous solution, Alex. Eng. J., 54 (2015) 1253–1263.
[45] A.H. Karim, A.A. Jalil, S. Triwahyono, S.M. Sidik, N.H.N. Kamarudin, R. Jusoh, B.H. Hameed, Amino modified mesostructured silica nanoparticles for efficient adsorption of methylene blue, J. Colloid Interface Sci., 386 (2012) 307–314.
[46] N. Gupta, A.K. Kushwaha, M.C. Chattopadhyaya, Adsorption studies of cationic dyes onto Ashoka (Saraca asoca) leaf powder, J. Taiwan Inst. Chem. Eng., 43 (2012) 604–613.
[47] K.V. Kumar, V. Ramamurthi, S. Sivanesan, Modeling the mechanism involved during the sorption of methylene blue onto fly ash, J. Colloid Interface Sci., 284 (2005) 14–21.
[48] M.U. Dural, L. Cavas, S.K. Papageorgiou, F.K. Katsaros, Methylene blue adsorption on activated carbon prepared from Posidonia oceanica (L.) dead leaves: Kinetics and equilibrium studies, Chem. Eng. J., 168 (2011) 77–85.
[49] P. Das, P. Banerjee, S. Mondal, Mathematical modelling and optimization of synthetic textile dye removal using soil composites as highly competent liner material, Environ. Sci. Pollut. Res., 22 (2015) 1318.
[50] S. An, X. Liu, L. Yang, L. Zhang, Enhancement removal of crystal violet dye using magnetic calcium ferrite nanoparticle: study in single-and binary-solute systems, Chem. Eng. Res. Design, 94 (2015) 726–735.
[51] M.A. Schoonen, J.M. Schoonen, Removal of crystal violet from aqueous solutions using coal, J. Colloid Interface Sci., 422 (2014) 1–8.
[52] R. Ahmad, Studies on adsorption of crystal violet dye from aqueous solution onto coniferous pinus bark powder (CPBP), J. Hazard Mater., 171 (2009) 767–773.
[53] T. Madrakian, A. Afkhami, M. Ahmadi, Adsorption and kinetic studies of seven different organic dyes onto magnetite nanoparticles loaded tea waste and removal of them from wastewater samples, Spectrochim. Acta Part A Mol. Biomol. Spectrosc., 99 (2012) 102–109.
[54] N. Dehghanian, M. Ghaedi, A. Ansari, A. Ghaedi, A. Vafaei, M. Asif, V.K. Gupta, A random forest approach for predicting the removal of Congo red from aqueous solutions by adsorption onto tin sulfide nanoparticles loaded on activated carbon, Desal. Water Treat., 57 (2016) 9272–9285.
[55] M. Ashrafi, M.A. Chamjangali, G. Bagherian, N. Goudarzi, Application of linear and non-linear methods for modeling removal efficiency of textile dyes from aqueous solutions using magnetic Fe_3O_4 impregnated onto walnut shell, Spectrochim. Acta Part A Mol. Biomol. Spectrosc., 171 (2017) 268–279.
[56] N. Goudarzi, D. Shahsavani, F. Emadi-Gandaghi, M.A. Chamjangali, Quantitative structure–property relationships of retention indices of some sulfur organic compounds using random forest technique as a variable selection and modeling method, J. Sep. Sci., 39 (2016) 3835–3842.
[57] K. Roy, S. Kar, R.N. Das, A primer on QSAR/QSPR modeling: Fundamental concepts Springer. 2015.
[58] V. Svetnik, A. Liaw, C. Tong, J.C. Culberson, R.P. Sheridan, B.P. Feuston, Random forest: a classification and regression tool for compound classification and QSAR modeling, J. Chem. Info. Comp. Sci., 43 (2003) 1947–1958.
[59] J. Li, Z. Shao, C. Chen, X. Wang, Hierarchical GOs/Fe_3O_4/PANI magnetic composites as adsorbent for ionic dye pollution treatment, RSC Adv., 4 (2014) 38192–38198.